

Authors' Response to Comments from anonymous referee #1

Black, italic: Referee's comments

Blue: Author's reply

Red: Changes in the original discussion paper

This manuscript the first measurements from an airborne instrument, UVHIS, which measures backscattered light in the UV and visible parts of the electromagnetic spectrum. It includes instrument characteristics and background, data processing/calibration steps, and results from a NO₂ VCD retrieval from its research flight near Feicheng, China. This paper fits the scope of AMT and would be a welcome read to the AMT audience for a new capability for high spatial resolution trace gas observations in a new region of the world. However, before publishing, this manuscript requires the addressing of technical corrections that cause some concern, expansion of details in places, and some improvement on the quality of the writing. While most the comments are minor and related to the writing, I do recommend revisions in the major category because of the concern about the VCD measurement (which may be correct but needs more details to describe to convince the reader) and a great expansion of the mobile DOAS description. Detailed comments on those are below.

First, we appreciate the overall positive response of the referee and we would like to thank for his constructive comments and helpful suggestions on the manuscript. As described below, we have modified the manuscript according to suggestions and provided clarifications where necessary.

1. There are concerns about the actual calculation of the NO₂ VCD as described in Sect 4.3. It is hard to tell what the VCD actually represents in the calculation. Is it a total column VCD? If so, the stratospheric details are missed. However, as it is stated that the stratospheric column is assumed stable during the flight from the reference and is canceled out leads the reader to believe it is not a total column. If it's just the below aircraft column, please state this and ensure the proper accounting for the distinction in the AMF and VCD calculation (e.g., Lamsal et al., 2017 is a great example that shows the breakdown of how these components are calculated).

In this manuscript, the NO₂ vertical columns we calculated are tropospheric vertical columns. We added necessary clarification throughout the manuscript. For example, we changed the title of the manuscript to 'The first high-resolution tropospheric NO₂ observations from the Ultraviolet Visible Hyperspectral Imaging Spectrometer (UVHIS)'.

2. Line 157-158: Pertaining to the spatial and temporal variability of the stratosphere being stable. This is maybe close to correct for a 3 hours flight, however there are changes in the SZA which will impact the slant column difference between the measurement and the reference. This

could be estimated with a geometric calculation of the slant path with an assumed stratospheric amount between the reference and the measurement. It likely is small.

According to TROPOMI L2 NO₂ product on 23 June, 2018, the NO₂ stratospheric vertical columns is about 3.5×10^{15} molec cm⁻² in flight area. The SZA of reference spectra is about 13°, while the largest SZA of 37° occurred in the end of 3 hour flight. Under simple geometric approximation of light path, the largest difference of SCD of stratospheric NO₂ between the measurement and the reference is about 8×10^{14} molec cm⁻².

3. Lines 306 and 288: The mean slant column fitting error of 4.8×10^{15} molecules cm⁻² and mean total value of error of 2.6×10^{15} molecules cm⁻² for the VCD column with a range going down to 1×10^{15} molecules cm⁻² does not seem to work out mathematically unless the AMF error is zero (which it is not) and the AMF must be ~ 2 (which is seems to be below that for most cases) and the error of the reference itself is 100% which is stated as 1×10^{15} . Please check this math.

We recalculated the NO₂ dSCD by adding a H₂O vapor cross section from HITRAN database, the mean slant column fitting error slightly decreased (still about 4.8×10^{15} molec cm⁻²). We modified the tropospheric NO₂ vertical column of reference spectra to 3×10^{15} molec cm⁻² with error of 1×10^{15} molec cm⁻² based on TROPOMI NO₂ product. We checked the AMF calculation, and the mean value of AMF during the flight is about 2. We also update the figure of time series of AMF, surface reflectance, SZA and RAA. After the recalculation, the mean total value of error is 3.0×10^{15} molec cm⁻² with a range from 1.5 to 5.9×10^{15} molec cm⁻².

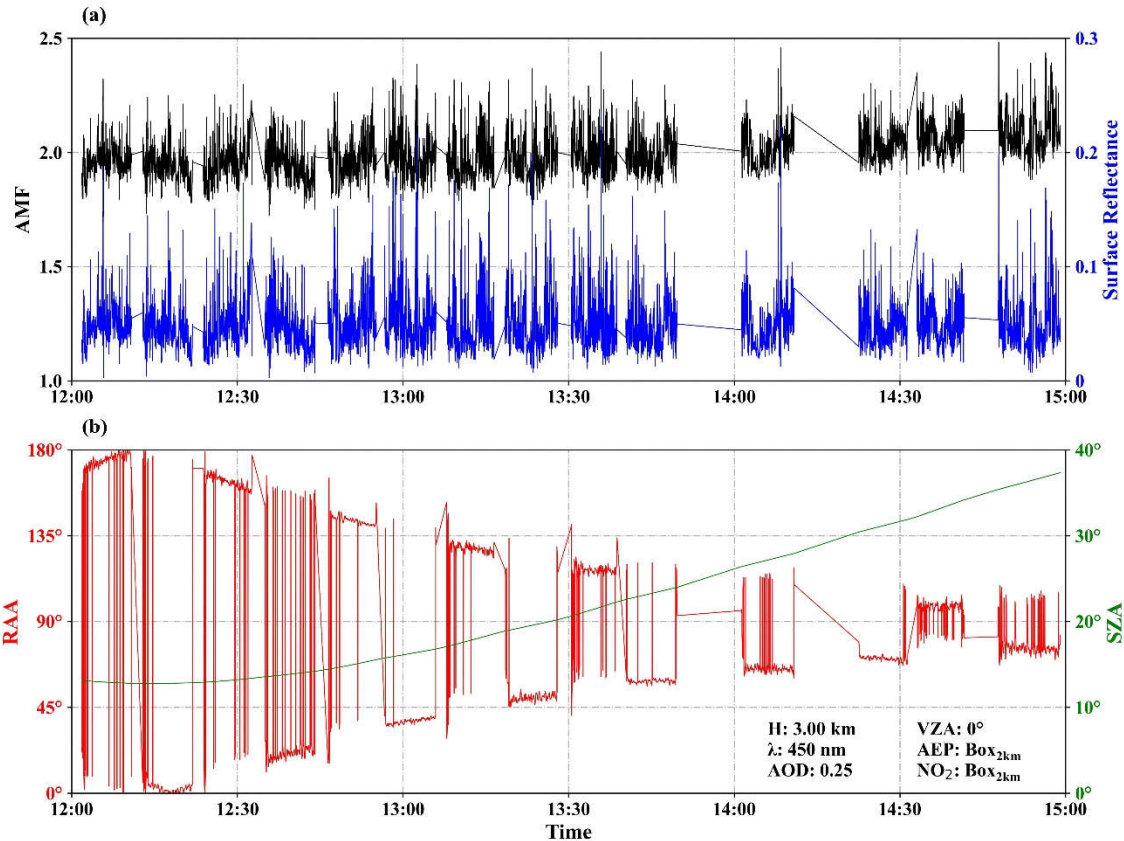


Figure 7. Time series of NO₂ AMF compared with (a) surface reflectance; (b) SZA and RAA for the research flight on 23 June 2018, computed with SCIATRAN model based on the RTM parameters from the UVHIS instrument. Only data of the nadir observations in each flight line are plotted.

4. Line 17: the error of 2.6×10^{15} is not the fitting error as stated. It is the error based on all sources of uncertainty.

Corrected.

Measurements of nadir backscattered solar radiation of channel 3 are used to retrieve tropospheric vertical column densities (VCDs) of NO₂ with a mean total error of 3.0×10^{15} molec cm⁻².

5. Are there literature references for the mobile-DOAS measurements? If not, then details on the specifics of that measurement need to be greatly expanded upon as well as the zenith-sky NO₂ retrieval in Sect 6.2. Especially details on the uncertainty and what the VCD represented vertically (just the troposphere? Stratosphere?).

We added two paragraphs in Sect 6.2 to describe the mobile DOAS tropospheric NO₂ retrieval method and its uncertainty analysis. For better comparison with UVHIS NO₂ observations,

assumptions and parameters in NO₂ retrieval method for the mobile DOAS were set to the same as the UVHIS.

For better comparison with UVHIS NO₂ observations, assumptions and parameters in NO₂ retrieval method for the mobile DOAS were set to the same as the UVHIS. For example, residual amount of NO₂ in reference spectra was set to 3×10^{15} molec cm⁻² with an error of 1×10^{15} molec cm⁻²; mobile DOAS observations only focus on tropospheric portion of NO₂ columns, assumed that the difference of the stratospheric NO₂ columns between observed spectra and reference spectra is negligible; vertical profiles of NO₂ and aerosol extinction, albedo, and aerosol properties in the AMF calculation were set to the same as UVHIS.

Like the uncertainty analysis of UVHIS NO₂ columns, the total uncertainty on the retrieved mobile tropospheric VCD is composed of three parts: (1) the mean uncertainty on dSCD of mobile DOAS is 1.4×10^{15} molec cm⁻²; (2) the uncertainty of reference vertical column is estimated to be 1×10^{15} molec cm⁻². In the case that the tropospheric AMFs of measured and reference spectra are very close, this part results an uncertainty 1×10^{15} molec cm⁻² to the total uncertainty; (3) the mean relative uncertainty on the AMF calculation is 22 % by square root of the quadratic sum of individual uncertainties like UVHIS. Combining these uncertainties together, the mean total uncertainties on the retrieved tropospheric NO₂ VCD is 2.1×10^{15} molec cm⁻².

6. In Figure 2, there are lines that are repeated in the northern half of the raster. Can this be described? Does this impact the comparisons to the mobile DOAS measurements? Please describe this overlap in the paper as this is what is shown in the NO₂ data. The details should be discussed in the paper.

Indeed, several flight lines are repeated in the northern part of flight area, but the spectral data of UVHIS are not recorded because of misoperation. Only spectral data of the flight lines over the steel factory are recorded, and the pass time of aircraft is 13:26 and 14:57 respectively. We added a paragraph and a figure to discuss this in detail. For impact on the comparison with mobile DOAS, see answer in question No. 22.

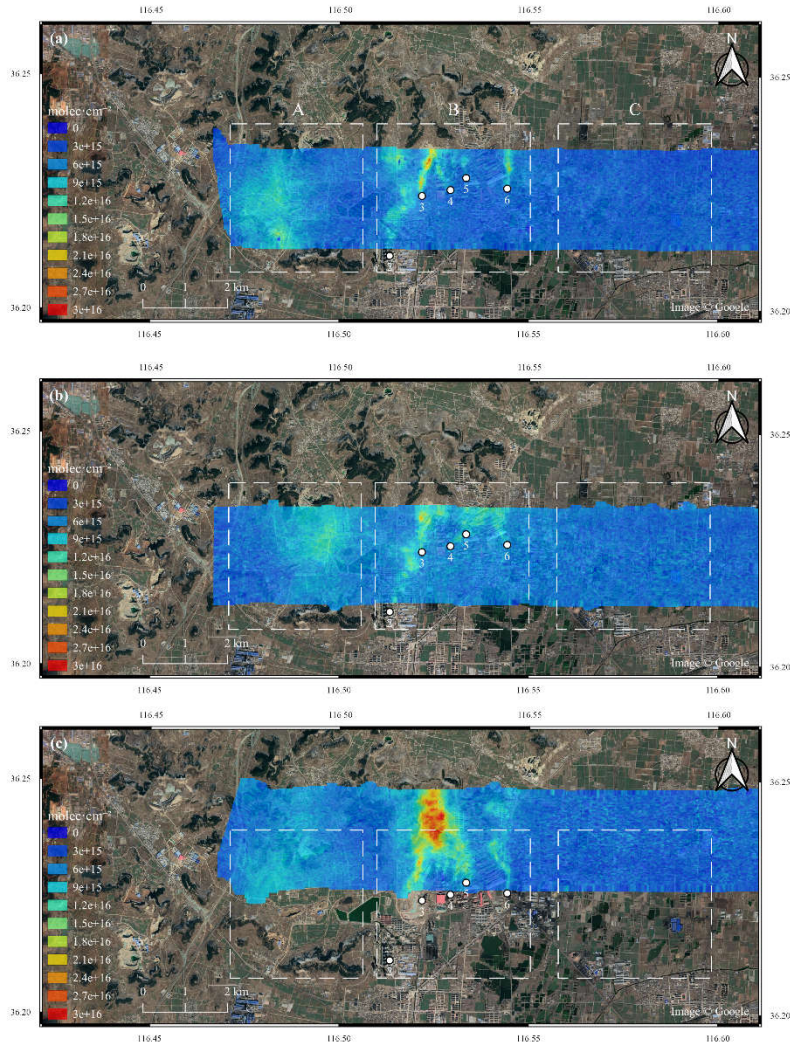


Figure 12. Three flight lines that pass through the steel factory, at local time 13:26 (a), 13:32 (c), and 14:57 (b). Panel (a) and (b) represent flight lines that cover the same area with a 1.5 hour time gap, panel (a) and (c) represent adjacent flight lines with a 6 minutes time gap.

Due to temporal discontinuity of flight lines and dynamic characteristics of NO_2 field, artefacts can be observed between adjacent flight lines. Figure 12 shows three flight lines that pass through the steel factory, at local time 13:26 (a), 13:32 (c), and 14:57 (b). Panel (a) and (b) represent flight lines that cover the same area with a 1.5 hour time gap, panel (a) and (c) represent adjacent flight lines with a 6 minutes time gap. These flight lines can be divided into three regions: region A covers no NO_2 source but is affected by carbon factories about 3 km away; region B covers the steel factory as dominant NO_2 source; region C covers no NO_2 source and is not affected by other sources. Compared to region B, there is a large temporal variety of NO_2 VCDs in region A between three flight lines. Region C is temporally consistent with relatively low NO_2 columns. From these observations it may be concluded that largest temporal variability could occur where there is no local NO_2 source but is down-wind of other sources, especially when wind direction is changing.

7. Line 108: The mobile DOAS measurements are not shown in Figure 5 as stated. However, are shown in Figure 11. Consider adding the location of these measurements in Figure 2 to show where the mobile DOAS measurements were taken. Additionally, in Lines 288-290: technical details about mobile DOAS measurements are not mentioned before this. Discuss these points within Sect 6.2.

We added the location of mobile DOAS measurements in Figure 2, and added technical details about mobile DOAS VCD retrieval method and its uncertainty analysis in Sect 6.2 as stated before.

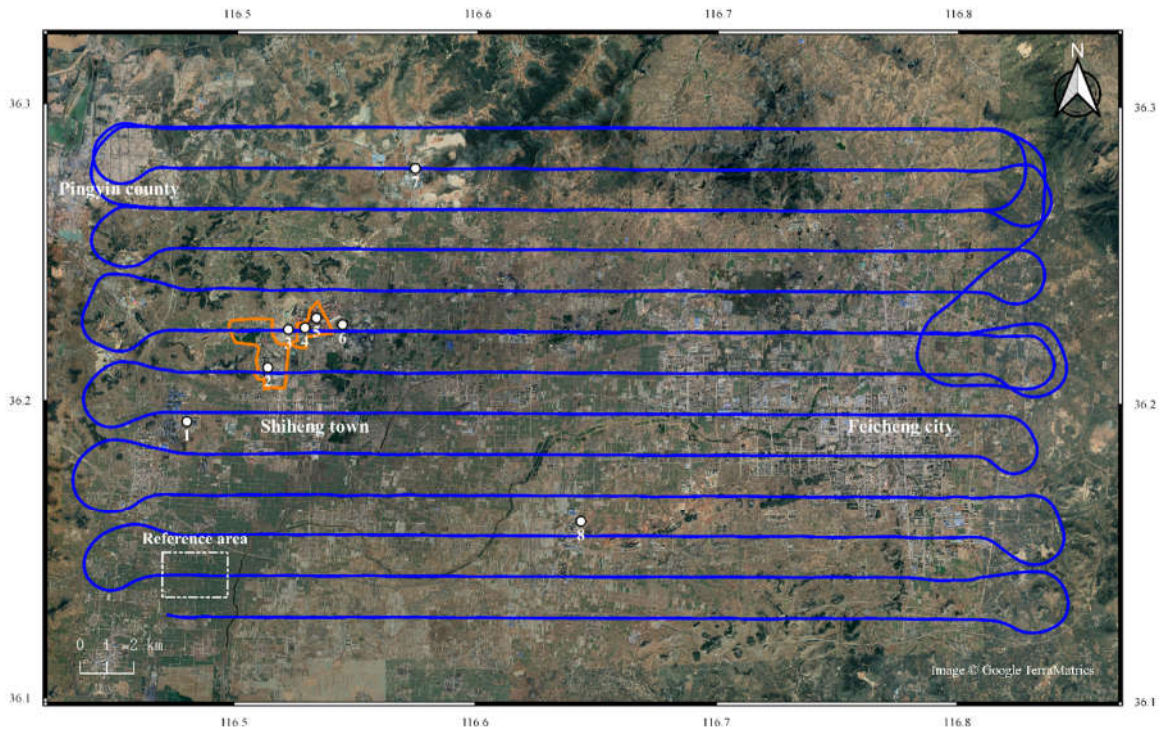


Figure 4. Overview of the Feicheng demonstration flight on 23 June, 2018. Flight lines are shown in blue. Two orange circles represent the routes of mobile DOAS system. White dots numbered from 1 to 8 represent the major emission sources. Number 1: several carbon factories; number 2: a power plant; number 3-6: individual emitters inside the steel factories, while number 4 and 5 are inside the circle of one mobile DOAS route; number 7-8: two cement factories. White dashed box represents the reference area.

8. Line 28: What is the intended meaning behind 'that NO_x attracts large attention'. Please elaborate with some details and examples.

Due to rapid industrialization and urbanization in the past few decades, China has become one of the largest NO_x emitters in the world. As a result, China is experiencing a series of severe air pollution problems. Therefore, measuring NO_x distribution by application of different techniques would benefit the pollutant emission detection and the air quality forecast. We modified this paragraph as below:

Nitrogen oxides (NO_x), the sum of nitrogen monoxide (NO) and nitrogen dioxide (NO₂), plays a key role in the chemistry of the atmosphere, such as the ozone destruction in the stratosphere (Solomon, 1999), and the secondary aerosol formation in the troposphere (Seinfeld and Pandis, 2016). In the troposphere, despite lightning, soil emissions and other natural processes, the main sources of NO_x are anthropogenic activities like fossil fuel combustion by power plants, factories, and road transportation, especially in the urban and polluted regions. As an indicator of anthropogenic pollution which leads to negative effects both on the environment and human health, the amounts and spatial distributions of NO_x attract large attention. For example, China becomes one of the largest NO_x emitters in the world due to fast industrialization, meanwhile China is also experiencing a series of severe air pollution problems in recent years (Crippa et al., 2018; An et al., 2019). Therefore measuring NO_x distribution by application of different techniques, would benefit the pollutant emission detection and the air quality trend forecast (Liu et al., 2017; Zhang et al., 2019).

9. Line 54: add 'of NO₂' after spatial distribution to clarify that this is the gas of interest in this paper.

Corrected.

10. Lines 67-68. Figure 1 only shows the optical bench for one of the channels and not all three as implied by the text. Please fix to the text saying that Figure 1 shows the optical bench for channel 3 and that the other two are similar.

Corrected.

Figure 1 shows the optical bench of channel 3 and that the other two are similar. The optical design of each channel comprises a telecentric fore-optics, an Offner imaging spectrometer, and a two dimensional charge-coupled device (CCD) array detector.

11. Line 86-87: reword this sentence to say that spectral and radiometric calibration in the laboratory were done prior to flights to reduce errors in spectral analysis. There shouldn't be a need to state it as 'very necessary'.

Corrected.

12. Line 38: Is this the first space-borne sensor ever in China or the first space-borne sensor related to air quality or trace gases?

The EMI is the first space-borne sensor related to trace gas monitoring, we corrected this in the manuscript.

13. Line 126: clouds were mentioned as filtered out. However, in the rest of the paper it says that the conditions were cloud free. Were there clouds to be filtered? If so, state where and how cloudy it was. If not, state that cloud filtering was not needed for these measurements due to clear skies. Same comment with the sun glint on water if applicable.

The weather condition is cloud free on 23 June, 2018. However, sun glint on water occurred several times in the southern part of flight area (especially over the river near the reference area) because of the low solar zenith angles. We add this statement in the manuscript.

The preprocessing procedure before spectral analysis includes data selection, dark current correction, spatial binning, and in-flight calibration. First, the spectral data acquired during U-turns of aircraft are removed in the processing because of the large and changing orientation angles. Also a threshold of radiance values is set to neglect some over-illuminated ground pixels inside the flight area, which are usually caused by presence of cloud or water mirror reflection. During the entire flight, sun glint on water occurred several times in the southern part of flight area, especially above the river near the reference area. However, cloud was not present due to clean clear-sky weather condition.

14. Line 165: Please revise to say something like 'and the properties that influence radiative transfer of light through the atmosphere' instead of 'and the radiative transfer'

Corrected.

15. Line 184: Please clarify which MODIS AOD product was used.

MODIS AOD product used in this paper is MYD04 on 23 June, 2018, with resampling for every ground UVHIS pixel. We added this in the manuscript.

(5) Aerosol optical Depth (AOD) information used in AMF calculation is MODIS AOD product MYD04 at 470 nm on the same day with resampling for every ground UVHIS pixel (Remer et al., 2005), because neither ground-based aerosol measurement is performed, nor any AERONET station data near the flight area is available.

16. Line 184: What was the AOD measured from MODIS was during the flight? Please add this detail into the manuscript.

MODIS AOD product used in this paper is MYD04 on 23 June, 2018, with resampling for every ground UVHIS pixel. We added this in the manuscript as stated before.

17. Line 187: Please justify why SSA of 0.93 and asymmetry factor of 0.68 are used.

The SSA and asymmetry factor of aerosol used in the manuscript are estimation of typical urban/industrial aerosols based on previous studies (Li et al., 2018).

Like the NO₂ profile, the aerosol extinction box profile is constructed from the PBL height and AOD. Single scattering albedo (SSA) is assumed to be 0.93, and asymmetry factor is assumed to be 0.68 for aerosol extinction profile, based on previous studies of typical urban/industrial aerosols (Li et al., 2018).

18. Line 226: Is [28] a referring to a reference? Please fix.

Corrected.

19. Consider consolidating Figures 6, 8, and 9 into one figure.

We added an AMF dependency analysis on the VZAs, also a new panel in Figure 8. As shown in Fig. 8 (b) and (c), the changes of AMF are 10% and 7% respectively, when other parameters are set as mean.

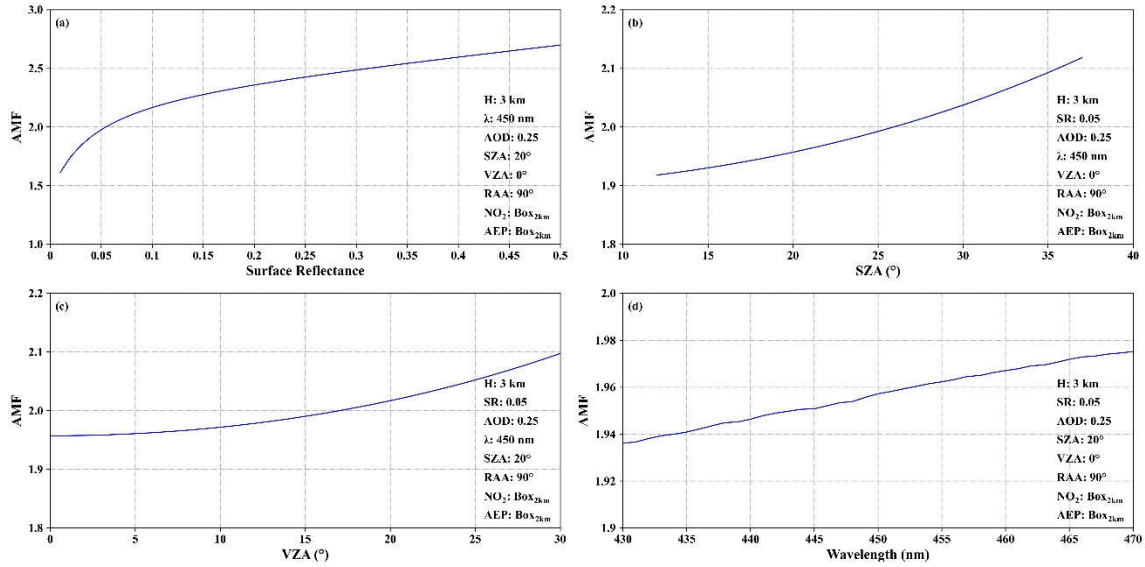


Figure 8. AMF dependence analysis results (a): on the surface reflectance; (b): on the SZAs; (c): on the VZAs; (d): on the wavelength.

20. Line 258: The difference in adjacent flight lines are not ‘biases’ but rather ‘artifacts’ of the changing NO₂ VCDs due to temporal variation.

Corrected.

21. Section 6 would benefit from a more descriptive title, like ‘NO₂ VCD Assessment’ rather than ‘Discussion’

We changed the title of Sect 6 to ‘NO₂ VCD Assessment’.

22. Lines 324-325. How do these results change if only considering points with a stricter temporal window between the mobile and aircraft measurements?

We added a new comparison to co-located mobile DOAS measurements only circled the steel factory, and the correlation coefficient improves to 0.86. In this case, all mobile measurements occurred inside the swath of one flight line of aircraft, and the time offset between instruments shortened to 15 minutes.

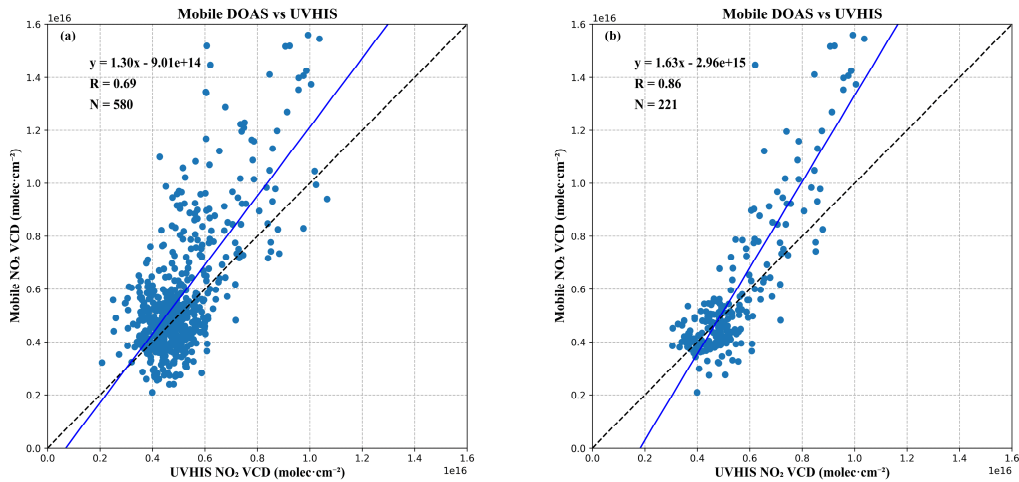


Figure 14. Scatter plot and linear regression analysis of the co-located NO₂ VCDs, retrieved from UVHIS and mobile DOAS system, (a) for all co-located measurements, (b) for co-located measurements that only circled the steel factory.

Figure 14 (a) shows scatter plots with VCDs retrieved by UVHIS on the x-axis and mobile DOAS VCDs on the y-axis, for all co-located measurements. The corresponding results of linear regression analysis are also provided in Fig.14 (a), with a correlation coefficient of 0.69, a slope of 1.30, and an intercept of -9.01×10^{14} . The absolute time offset between mobile DOAS and airborne observations can be up to 1 hour, which means that both instruments cannot sample the NO₂ column at certain geolocation simultaneously. As shown in Fig. 14 (b), when only comparing UVHIS VCDs to mobile measurements that circled the steel factory, the correlation coefficient improves to 0.86. In this case, all mobile measurements occurred inside the swath of one flight line of aircraft, and the time offset between instruments shortened to 15 minutes. In general, an underestimation of UVHIS VCDs of increased value can be observed in Fig 14 (a) and (b). Considering the variability in local emissions and meteorology, it is reasonable that the differences between these two instruments exist. Besides, the averaging effect of the area inside an UVHIS pixel can also lead to the underestimation of UVHIS compared to mobile DOAS system.

23. In line 323, the difference between the mobile DOAS measurements and the airborne measurements is described as an ‘overestimate’ of mobile DOAS measurements, but in the conclusions and abstract it is stated as an ‘underestimate’ by the aircraft. Please be consistent in this description in the manuscript.

Corrected.

24. Figure 2: the black dots are hard to see. Please change the color and/or symbol to make the points of interest stand out.

We updated Figure 2 as stated before.

25. Instead of having Table 2, could those results be translated into Figure 3(a) somehow? If keeping Table 2, then be more descriptive in the caption to say these are FWHMs at these wavelengths/angles.

We added more information in the title of Table 2, also we added a new figure to plot the slit function shapes of 9 viewing angles at 450.504 nm.

Table 2. Preflight wavelength calibration results (FWHMs) of UVHIS channel 3 for 9 viewing angles. Light sources used in the calibration are a mercury-argon lamp and a tunable laser. Slit function shapes are retrieved by least square fitting of characteristic spectral lines, using a symmetric Gaussian function.

FOV	379.887 nm	404.656 nm	450.504 nm	500.566 nm
-20°	0.35 nm	0.35 nm	0.39 nm	0.50 nm
-15°	0.33 nm	0.31 nm	0.33 nm	0.43 nm
-10°	0.31 nm	0.29 nm	0.29 nm	0.41 nm
-5°	0.31 nm	0.30 nm	0.29 nm	0.34 nm
0°	0.31 nm	0.32 nm	0.30 nm	0.30 nm
5°	0.34 nm	0.36 nm	0.34 nm	0.30 nm
10°	0.38 nm	0.39 nm	0.38 nm	0.32 nm
15°	0.40 nm	0.44 nm	0.42 nm	0.35 nm
20°	0.45 nm	0.46 nm	0.47 nm	0.38 nm

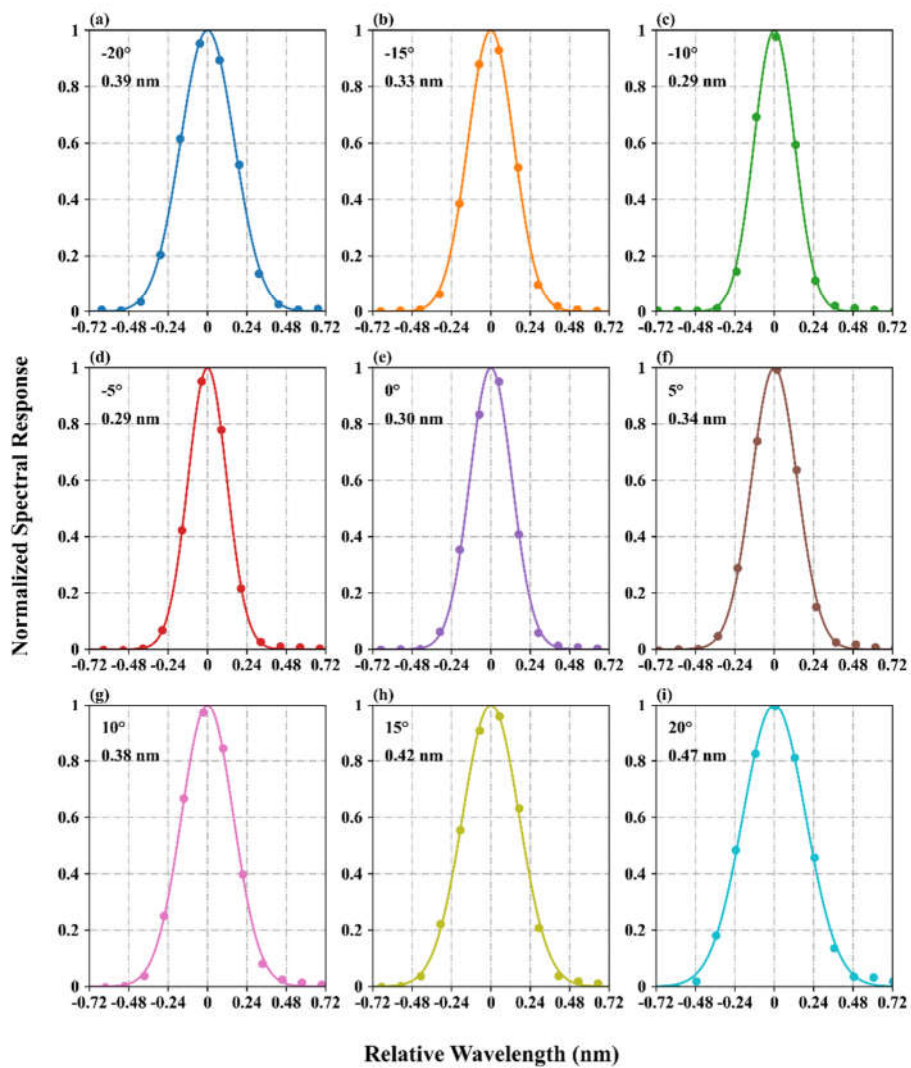


Figure 2. Measured slit functions (dots) at 450.504 nm and retrieved slit function shapes (lines) using a symmetric Gaussian function for 9 viewing angles.

26. Lines 110-113: This text is redundant. These details were already stated in the previous paragraph.

We reorganize this paragraph as below:

In the condition of spatial binning by 10 pixels across-track, the across-track spatial resolution of the ground pixel is about 22 m. At typical aircraft ground speed of 50 m/s and integration time of 0.5 s, the along-track spatial resolution of the ground pixel is about 25 m.

27. Similarly, the first two paragraphs in Section 5 appear to be redundant. Please consolidate into one paragraph without repeating details already stated.

We reorganize Sect 5 as below:

The NO₂ tropospheric VCD two-dimensional distribution map is shown in Fig. 10 for the research flight on 23 June 2018. With a high performance of UVHIS in spectral and spatial resolution, Figure 10 shows fine-scale NO₂ spatial variability to resolve individual emission sources. In general, the NO₂ distribution is dominated by several exhaust plumes with enhanced NO₂ concentration in the northwest part, which share a transportation pattern from south to north consistent with the wind direction. These sources include a power plant, a steel factory, two cement factories, and several carbon factories. The largest plume with peak values of up to 3×10^{16} molec cm⁻², originates from an emitter inside a steel factory (number 3 in Fig. 10). This dominant plume reaches its peak value outside at a small valley about 1 km north of the factory, and is transporting at least 9 km and seems to be continuing outside the flight region. This enhanced level of NO₂ may be caused by terrain factor which contributes to the accumulation of pollution gases.

Number 4 to 6 represent other emitters inside the steel factory. While the exhaust plumes originated from number 4 and 5 merge with the dominant plume, the plume from number 6 transports to north individually with a peak value of 1.4×10^{16} molec cm⁻². A weaker plume with peak values of 1.5×10^{16} molec cm⁻² is also detected by UVHIS, which seems to originate from the power plant. Indicated by number 2 in Fig. 10, this power plant is less than 2 km south of the steel factory. Number 1 in Fig. 10 indicates several carbon factories, which are located on the left side of the flight area. Several plumes with peak values of 1.5×10^{16} molec cm⁻², gradually merge together during transportation downwind. Number 7 and Number 8 in Fig. 10 represent two different cement factories. Peak values of these two plumes are 1.5×10^{16} molec cm⁻² and 1.4×10^{16} molec cm⁻² respectively.

Compared to the industrial areas mentioned above, the pollution levels of the rural areas are much lower due to the lack of contributing sources, ranging from 2 to 6×10^{15} molec cm⁻². The urban area of Feicheng city is located on the right side of the flight area. Figure 11 is an enlarged map of UVHIS NO₂ observations over Feicheng city, with a color scale only extends to 7×10^{15} molec cm⁻². Two black lines in Fig. 11 represent the truck roads in this city. The S104 is a provincial highway that crosses Feicheng from north to south, while the S330 crosses Feicheng from east to west. Although lots of noise can be observed in Fig. 11, the NO₂ sources in Feicheng are mainly related to traffic and concentrated along the S104.

Due to temporal discontinuity of flight lines and dynamic characteristics of NO₂ field, artefacts can be observed between adjacent flight lines. Figure 12 shows three flight lines that pass through the steel factory, at local time 13:26 (a), 13:32 (c), and 14:57 (b). Panel (a) and (b) represent flight

lines that cover the same area with a 1.5 hour time gap, panel (a) and (c) represent adjacent flight lines with a 6 minutes time gap. These flight lines can be divided into three regions: region A covers no NO₂ source but is affected by carbon factories about 3 km away; region B covers the steel factory as dominant NO₂ source; region C covers no NO₂ source and is not affected by other sources. Compared to region B, there is a large temporal variety of NO₂ VCDs in region A between three flight lines. Region C is temporally consistent with relatively low NO₂ columns. From these observations it may be concluded that largest temporal variability could occur where there is no local NO₂ sources but is down-wind of other sources, especially when wind direction is changing.

28. There are grammar mistakes throughout the manuscript. These errors will need to be fixed before publication but I expect will be evolving in revisions. Some grammar and other writing fixes are located at the bottom of this review to help give examples as to the types of errors found. They are not a full edit.

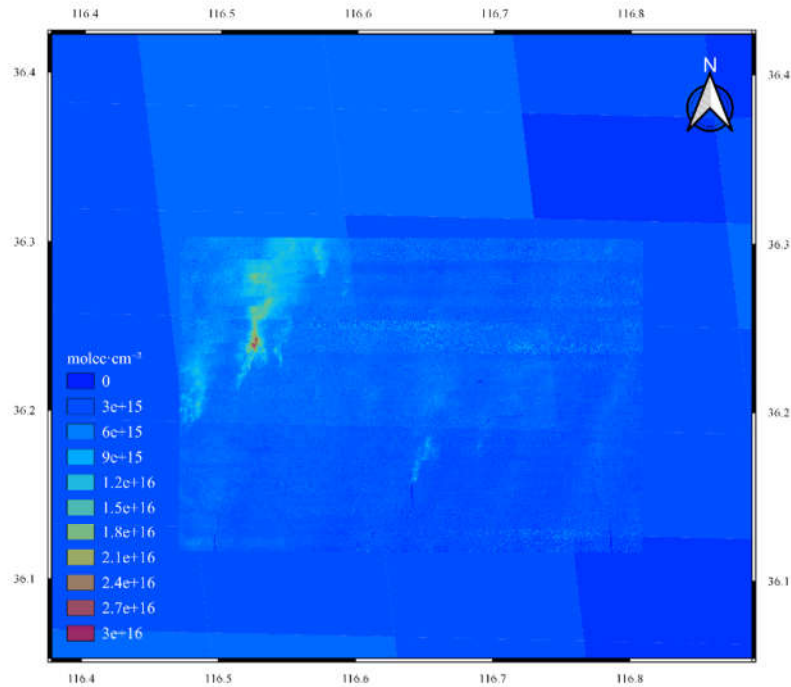
Corrected.

29. Consider a more concise title, such as, 'The first high-resolution NO₂ observations from the Ultraviolet Visible Hyperspectral Imaging Spectrometer (UVHIS)'.

We changed the title of the manuscript to 'The first high-resolution tropospheric NO₂ observations from the Ultraviolet Visible Hyperspectral Imaging Spectrometer (UVHIS)'.

30. Does EMI capture this area? Or TROPOMI? It would be interesting to show some comparisons to those data products, especially since the flight was early afternoon on a cloud free day.

Both EMI and TROPOMI capture this area on 23 June, 2018. In the figure below, we plot TROPOMI tropospheric NO₂ vertical columns because of its high spatial resolution. A quantitative comparison of the two retrievals may not make much sense because we use TROPOMI product to estimate the reference residual. However, enhancements in TROPOMI NO₂ are consistent with large UVHIS columns inside the flight area. Also, enhancements in TROPOMI NO₂ columns to the north of the flight area may indicate that the plumes originated from the steel factory keep transporting for tens of kilometers.



31. What does Feicheng City look like if mapped on a color scale that only extends to 5×10^{15} . Are there spatial patterns captured? It is hard to see any patterns in Figure 10 in that area due to the color scale expanding to much larger pollution scales. Perhaps a second panel in this figure would be interesting.

We added a new figure of enlargement of UVHIS NO_2 VCD map over Feicheng city as below. More details can be found in answer to question No. 27.

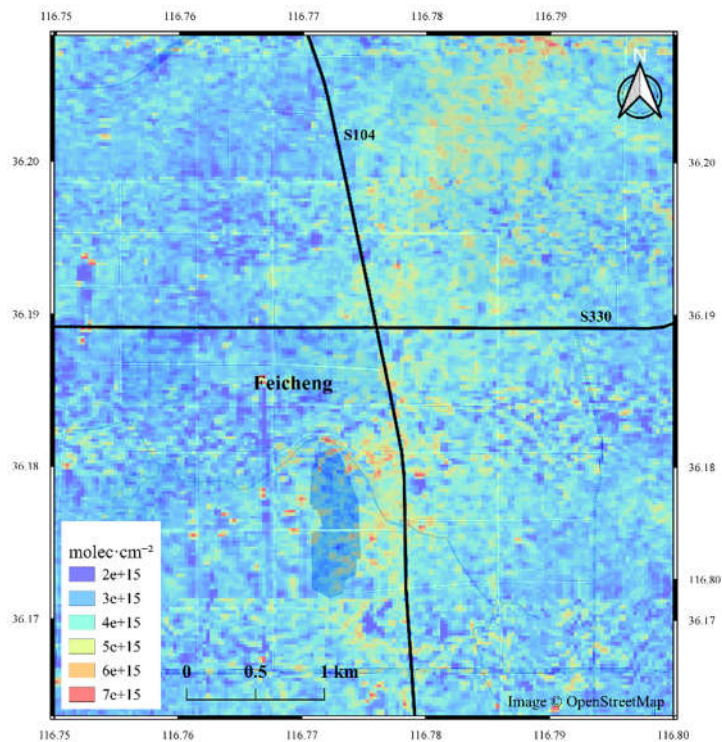


Figure 11. Enlargement of UVHIS NO₂ VCD map over Feicheng city with a color scale only extends to 7×10^{15} molec cm⁻². Two black lines in the map represent two truck roads that cross Feicheng city: S104, and S330.

32. *Figure 7: consider adding a true color image of this line to compare with the surface reflectance and AMF.*

For better comparison with surface reflectance and AMF, we added a panel in Figure 9 of radiance measurements from UVHIS. It is obvious that all panels share a same spatial distribution. However, some small differences can be observed due to time offset and spatial resolution difference.

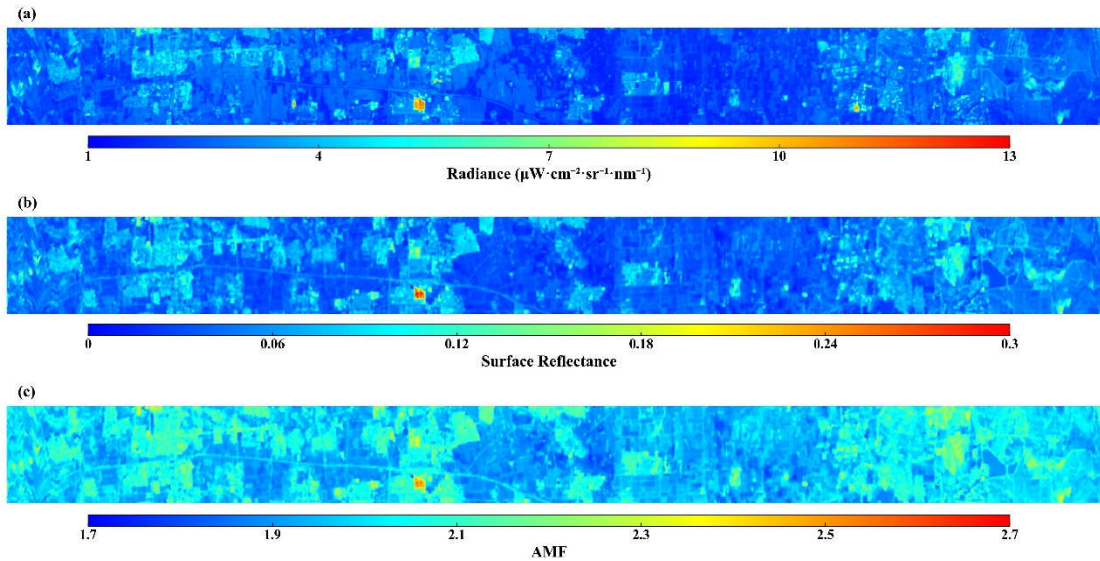


Figure 9. (a) UVHIS Measured radiance; (b) Landsat 8 Surface reflectance; (c) computed AMFs, for one flight line of the Feicheng data set. A strong dependency of the AMF on the surface reflectance can be observed.

33. *Can you comment on applications of the other channels for UVHIS? Are there plans for other products in the future?*

The UVHIS is part of a full spectral multimodal airborne imaging spectrometer. Our works only involve the channel 2 and 3 for trace gas measurements. In future works, we will present the retrieval results of SO_2 or HCHO based on measurements of channel 2. For channel 1 that covers deep UV spectral range, it is beyond our scope of work, and it may be used for wildfire or other artificial UV light source detection.